# *The Determination of a Cost Optimal Design for a Multiple Stage Continuous Electrodialysis Desalination Device for Use in Domestic Point of Use Water Purification*

**Proceedings of the ASME 2020**
**International Design Engineering Technical Conferences**
**and Computers and Information in Engineering Conference**
**IDETC/CIE2020**
**August 17-19, 2020, Virtual, Online**

**DETC2020-22670**



# THE DETERMINATION OF A COST OPTIMAL DESIGN FOR A MULTIPLE STAGE CONTINUOUS ELECTRODIALYSIS DESALINATION DEVICE FOR USE IN DOMESTIC POINT OF USE WATER PURIFICATION

**Hannah M. Varner[1], Sahil R. Shah[1], Amos G. Winter[1]**

[1]Massachusetts Institute of Technology, Cambridge, MA

## ABSTRACT

*There is a large and growing demand for point of use (POU) water desalination in emerging economies, such as India, where there is a large reliance on brackish (saline) groundwater reservoirs to meet drinking needs. In this work we propose a design for a two-stage continuous ED system that addresses the requirements of the Indian market while providing a higher water recovery than existing POU reverse osmosis products. Optimization was applied to minimize capital cost while ensuring 90% recovery of the feed, 90% salt reduction, and 15 L/hr of desalinated water production. The optimized design had a capital cost of approximately US$ 106, which is below the retail price of current RO purifiers on the market. Therefore, two-stage continuous ED shows promise for being a cost-competitive but water-efficient alternative to POU RO in India.*

Keywords: Electrodialysis, cost constrained, desalination, point of use

## NOMENCLATURE

| | |
|---|---|
| $C_{conc}$ | Concentration of concentrate channel |
| $C_{bulk,dil}$ | Bulk concentration of diluate channel |
| $C_{wall,dil}$ | Wall concentration of diluate channel |
| $E_{el}$ | Potential drop across electrode [V] |
| $E_{mem}$ | Potential drop across membranes [V] |
| $f$ | Friction factor |
| $h$ | Channel height [m] |
| $i_{lim}$ | Limiting current density [A/m$^2$] |
| $L$ | Flow path length [m] |
| $N\#$ | Number of cell pairs in stage number: # |
| $P$ | Pressure |
| $Q_{cp}$ | Cell pair volumetric flow rate |
| $R_c$ | Concentrate resistance [Ω-m$^2$] |
| $r_{ilim}$ | Maximum ratio of applied to limiting current |
| $R_{mem}$ | Membrane resistance [Ω-m$^2$] |
| $u_v$ | Void channel velocity |
| $V\#$ | Voltage applied to stage number: # |
| $W$ | Flow path width [m] |
| $\rho$ | Density of feed water |

## 1. INTRODUCTION

### 1.1 Motivation

Throughout much of the developing world, access to safe reliable drinking water remains a challenge as it is often intermittently available, biologically contaminated, or too saline to drink [1]. Brackish groundwater constitutes a majority of the accessible fresh water in the world, and is an underutilized resource that is becoming more important to meet growing water needs in water scarce regions. The motivating case study in this work is domestic water needs in urban India. Domestic point of use (POU) water purifiers are found in homes across India, and the market is predicted to grow by over 14% from 2018 to 2023 [2]. However, current point of use (POU) reverse osmosis (RO) products operate at low energy efficiency and water recovery, retaining only 30% of the incoming water as product and rejecting the rest as waste [3]. ED offers comparable energy efficiency with the possibility of conserving up to 90% of the feed water [4].

In the Indian domestic context, water is typically derived from one of a selection of sources, with higher cost and lower quality options (including tanker truck delivery or local surface water) supporting more expensive (bore well) or higher quality but intermittent supplies (e.g. municipal water) as needed to supply consistent water delivery to the home [5]. All these sources fall under 5000 mg/L total dissolved salts (TDS), the salinity threshold where ED delivers comparable water quality with reduced energy consumption and water waste to RO [1]. This indicates ED is a prime candidate to enter the POU desalination market, especially as Indian consumers and

governments become more concerned with water conservation [6,7].

POU purifiers are a consumer product; hence, low manufacturing capital cost is a key driver to ensuring uptake. The average POU purifier in India cost US$158 in 2018 [2]. While the primary customers in India tend to be upper middle-class households with higher income levels, capital cost remains the most important factor in whether a device will be successful when considering the design of an ED system for Indian POU application.

### 1.2 Electrodialysis Devices

Electrodialysis is a membrane desalination process in which salt transport is driven by applying an electric potential as shown in Figure 1. Saline feed water flows between a pair of electrodes. The applied current acts on charged ions, moving cations and anions in opposite directions. Selectively permeable membranes separate the flow into a diluate stream (with reduced ion content) and a saline brine stream.

Previous work has demonstrated the feasibility of implementing ED within domestic purifiers when operated to deliver water in batches to a storage tank [8,9]. However, while this system could meet the required water production rate at quality, there are disadvantages to the batch architecture. First, it requires more valving to enable voltage reversal (which decreases membrane scaling). The tanks required for batch operation require significant volume. Most importantly, the user experience is unfamiliar to current users; a batch system does not provide a continuous supply of desalinated water. Industrial implementations of ED frequently operate with a continuous production of water, achieving a target salinity through staging multiple modules in series, however this architecture has not been examined for POU applications [10].

Given this gap, we present in this paper a design for a two-stage **continuous** ED stack and system architecture that is optimized for minimum capital cost. The questions we address are:

1) How can the architecture of an ED stack and system be reimagined to reduce capital cost?
2) What is the cost optimal continuous stack design that satisfies the functional requirements for the POU application?
3) How can the design space be visualized with respect to imposed constraints in order to better understand future areas of design flexibility? And finally,
4) What are the limitations of the proposed design?

We first provide a brief overview of the ED process (Section 2.1) and the proposed system design (Section 2.2), before delving into our methodology for sizing the system for minimum cost (Section 3). Finally, we discuss the derived design and discuss the questions described above (Section 4).

## 2. PROPOSED SYSTEM DESCRIPTION

### 2.1 Electrodialysis Overview

A full ED module or 'stage' is comprised of repeating units of flow channels sandwiched between *ion exchange membranes* with alternating selectivity. This unit is called a *cell pair* and consists of one cation exchange membrane (CEM) and one anion exchange membrane (AEM). In Figure 1a, it can be seen that in the presence of an applied potential, ions in saline water will move towards the anode or cathode until they encounter an ion exchange membrane selective for the opposite charge. As a result, ions are driven out of the product (diluate) water and accumulate in the concentrate stream, which is rejected as brine.

An important parameter in ED is the limiting current density, $i_{lim}$ [A/m$^2$]. This is the diffusion-limited rate of ion transport. Current densities greater than $i_{lim}$ cause ion depletion at the membrane-diluate interface as shown in Figure 1b. Once the boundary layer is depleted of ions water-splitting begins to occur, which decreases system efficiency and can promote scale formation. In order to avoid these phenomena, conventional ED operation requires that $i < i_{lim}$. This is often implemented by requiring that the ratio of applied to limiting current density not exceed $r_{ilim}$ the maximum allowable ratio.

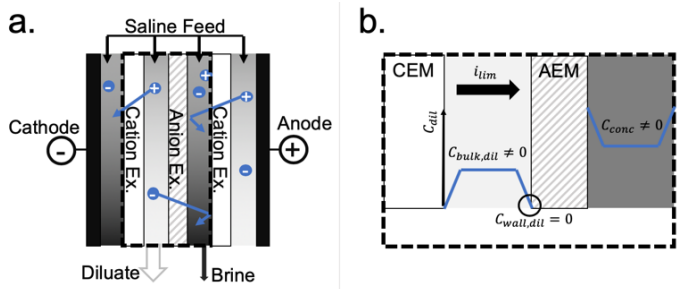


**FIGURE 1:** Alternating selectively permeable membranes enable ion collection and depletion within the flow during operation **a.** Cell pairs (denoted by the dotted line) consist of selectively permeable cation exchange membranes (CEM) and anion exchange membranes (AEM). Positioning these pairs between an anode and cathode facilitates the separation of ions from the saline feed. **b.** The applied current creates regions near the membranes where the salt concentration is significantly lower than the bulk.

Diluate concentration decreases over the length of the flow path, resulting in a proportional decrease in $i_{lim}$ (Figure 2a). Region I, above $i_{lim}$, falls outside of the operational limits of the system due to the water splitting phenomenon discussed above. By imposing a safety threshold $r_{ilim}$, we also prevent operation in Region II. The solid line represents desalination at a voltage, V. This voltage is therefore limited by the maximum applied current at the lowest concentration of the stage. This imposed limit results in a large amount of wasted desalination potential (Figure 2a region III) where the concentration could enable higher currents to be applied. Higher applied current density is desirable because it results in more efficient use of the ion exchange material, driving material needs lower and material costs down.

## 2.2 System Description

### 2.2.1 Proposed Two-Stage Continuous Stack

In this analysis we examine a 2-stage configuration where the applied potential can be independently controlled for two sequential stages (Figure 2b). It can be seen in Figure 2b that the area of region IV is increased by the addition of a second stage. This achieves the goal described above of operating with the applied current closer to $i_{lim}$ as a way to increase efficiency.

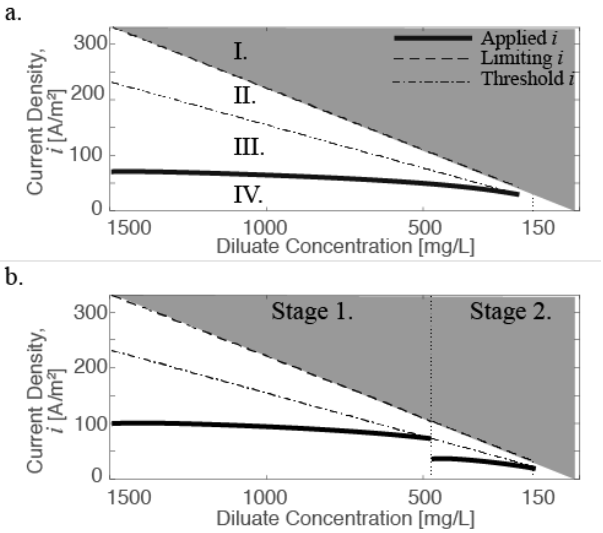


**FIGURE 2:** Current densities of interest over the course of desalination **a.** For a single pass through the ED stack, the limiting current density (and corresponding 0.7 safety factor threshold) decrease in the diluate stream. The maximum current that can pass through a stack can be seen to be limited by the region of lowest diluate concentration, occurring at the end of the flow path. Region I is masked given that $i_{lim}$ is exceeded in this region **b.** Adding two stages with independently controlled voltages allows the system to achieve higher desalination without reaching the limiting applied current density.

An additional strategy to reduce capital is proposed through a sharing of the center electrode between both hydraulic stages of the design (Figure 3a). Different field strengths can be applied to each hydraulic stage using the two additional electrodes at the ends of the stack. Within each stage, the number of cell pairs $N$ are further allowed to vary between the two stages, therefore allowing for different flow channel velocities in each hydraulic stage. However, the length of the water flow path, $L$, and the channel width, $W$, (Figure 3b) are held constant to decrease the number of different components in the assembly. The shape of the flow path seen in Figure 3b is made possible through the addition of a flow spacer that includes gasket area to prevent water flow outside of the specified region.

### 2.2.2 System Architecture

The two-stage stack described above would be a single component of the POU water purification system, analogous to the RO filters used in current systems. Figure 4 depicts how this stack would be positioned into the purifier architecture.

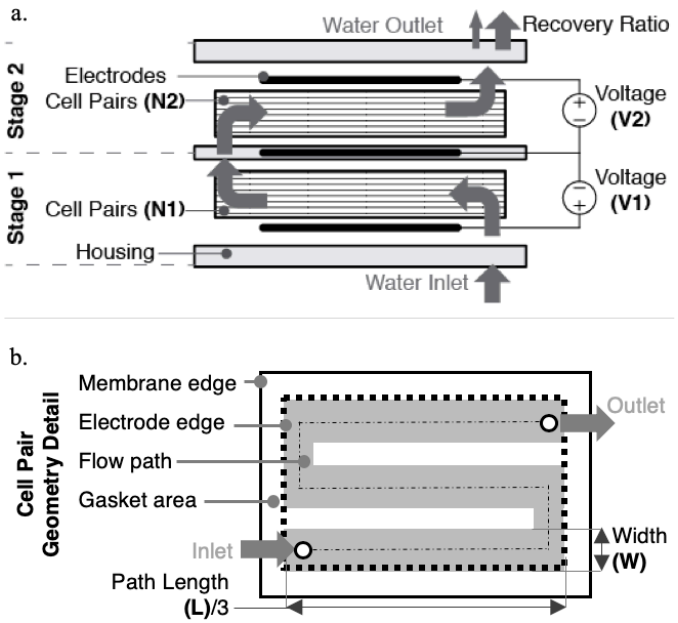


**FIGURE 3: a.** Sharing the center electrode in a two- stage stack reduces capital cost of the system. The water flow direction is mirrored from the first to the second stage. Bolded items (N1, N2, V1, V2) are variable parameters of the system. **b.** Within a single cell pair, the flow path is torturous in order to conserve area. The membrane and spacer have the same outer edge but the electrode is only required in the area of water flow.

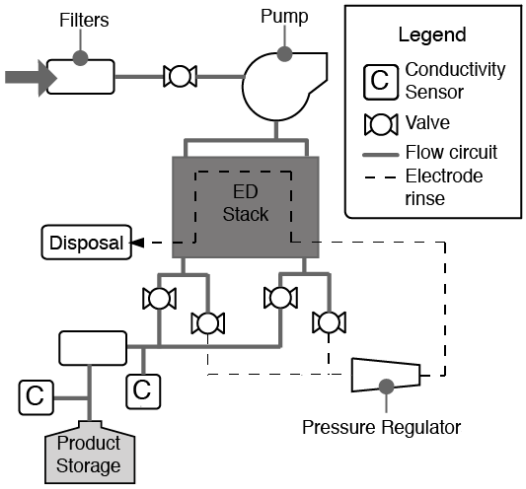


**FIGURE 4:** The two-stage stack relies on a pressure regulator on the outlet to achieve recovery over 50%. The stack performs the desalination step of the purification process and is supported by additional filters, valves and pumping systems.

For this design it is assumed that the recovery ratio is achieved by assuming the flow rate in the brine and diluate channels are independent. This is in contrast to the industrial norm of a feed-and-bleed system that maintains equal flow rates by recirculating brine in order to preserve volume but allow for water recovery over 50%. The independent flow rates could be

achieved in practice through inclusion of a flow restrictor on the brine outlet to apply a back pressure that would slow brine flow.

## 3. DESIGN OPTIMIZATION

### 3.1 Objective Function and System Constraints

This section presents the optimization of a two-hydraulic, two-electric stage continuous ED system with for minimum capital cost. ED stack costs include fixed costs (housing, power supply, flow fixtures) and variable costs. Analysis by Nayar et al. predict that 91% of the module cost is due to ion exchange membrane and electrode costs alone [8], therefore these were the two costs considered in estimating capital costs in this analysis. Total area of the membrane and electrode was calculated from the specified flow path *L* and *W* plus additional material around the path that gasket to prevent water leaking from the channel (Figure 3b).

The constraints applied to the design search were chosen to facilitate the viability of the unit as a consumer product in the Indian market. Table 1 lists the constraints considered in this design, along with a brief rational for each item. Throughout simulated operation, voltage applied to each stage was allowed to vary in order to increase the applied current density.

**TABLE 1.** Constraints and assumptions used in the system optimization.

| Parameter | Value | Justification |
|---|---|---|
| *Optimization Constraints* | | |
| Voltage | < 24 V | Typical power supply present in existing POU purifiers |
| Pressure drop | < 1 bar | Allow for small, low cost and low electrical consumption pumps to be used |
| $r_{ilim}$ | < 0.7 | Industry standard recommendations and previous work in the region [11,12] |
| *Inputs to the Optimization* | | |
| Feed salinity | 1500 mg/L | Accommodate the groundwater salinity over a majority of India [13] |
| Salt reduction | 90% | Salinity comparable to the maximum seen across packaged bottled water available in India [14] |
| Water recovery | 90% | Highly optimistic target provides a conservative (upper bound) cost estimate |
| Flow rate | 15 LPH | Typical production rate of commercial POU RO systems in India |

### 3.2 Models

When considering the overall design of an ED module, the fraction of salt removed from the feed depends on three factors: the residence time of the water within the system, how well the diluate channel is mixed, and the strength of the applied electric potential.

Analysis of the ED process for a given geometry was performed by leveraging previous work by Wright et al. that was modified to reflect continuous flow with varied flow velocities between diluate and brine channels [15]. Salinity was modeled as consisting of only monovalent NaCl ions, which was shown in the same work to be a reasonable approximation at a first pass for analyzing ED stacks. Properties of the key parameters used in the modeling are summarized in Table 2.

Voltage and pressure drop are of particular interest in this study; hence, the relevant equations are summarized here. The voltage drop across each stage was estimated using:

$$V = E_{el} + N[E_{mem} + i(R_d + R_c + R_{mem})] \quad (1)$$

The pressure drop is predicted from the Darcy-Weisbach equation of flow between two parallel flat plates:

$$\Delta P = \frac{\rho f L u_v^2}{4h} \quad (2)$$

The friction factor was determined using the method of Ponzio et al. [16] based on the Reynolds number calculated using the void channel velocity, $u_v$ (without spacer porosity included).

**TABLE 2.** Parameters of the spacer used in simulation.

| Parameter | Value | Justification |
|---|---|---|
| *Spacer characteristics* | | |
| Channel Height *(h)* | 0.350 mm | Parameters of commercial unit: PCCell GmbH (Heusweiler, Germany), model 64-002 |
| Open-Area Fraction | 0.6 | |
| Estimated Void Fraction | 0.62 | |
| *Membrane characteristics* | | |
| Resistance ($R_{mem}$) | 40 Ω-cm$^2$ | Experimentally determined safety factor over values reported by Ortiz et al. [17] |
| Potential drop ($E_{mem}$) | *Calculated* | Summation of the junction and Donnan potentials [18] |
| Cost per m$^2$ | US$40 | Previous quote [19] |
| *Electrode characteristics* | | |
| Potential drop ($E_{el}$) | 1.4V | Known metric for redox reaction occurring |
| Cost per m$^2$ | US$40 | Previous quote [20] |

### 3.3 Design Domain

The minimum capital cost design was determined through a scatter search. In structuring the simulations, geometric properties of the path were varied through specified ranges and the model described above was used to calculate the voltage required in each stage to achieve the desired salt reduction (Figure 5). The resolution for the widths was chosen based on limitations of the fabrication process of flow spacers within the lab setting where widths have been demonstrated to be controlled within 2 mm.

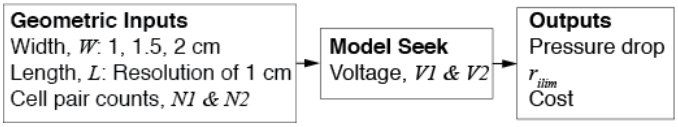


**FIGURE 5:** Geometric inputs are selected over a range of inputs and fed to the computational model that returns system characteristics of interests for each design. Width was resolved at 0.5 cm from 1.5 to 2.5 cm; length was resolved at 1 cm from 40 to 60 cm; N1 was assessed from 8 to 22 cell pairs; N2 from 6 to 11 cell pairs for N1=13 and rescaled as necessary for N1 values at extremes of the range.

#### 3.3.1 Determination of Salinity Targets

The product salinity $C_{prod}$ and intermediate salinity $C_{int}$ were both specified as inputs to the model. The intermediate salinity

was fixed as the geometric mean of $C_{feed}$ and $C_{prod}$ as described by Equation 3. This was determined analytically from methodology similar to that presented by Shah et al. [21] and modified to assess the desalination potential in a single pass through the continuous system. Further details of this analysis can be seen in Appendix 1. This analytical method was validated using the system simulation in Section 4.5.

$$C_{int} = \sqrt{C_{feed} C_{prod}} \quad (3)$$

## 4. RESULTS AND DISCUSSION

### 4.1 Optimal Design

The minimum capital cost design that satisfied all constraints specified in Table 1 had a capital cost of $US 106 (membranes and electrodes only). Table 3 summarizes the width and length of the flow path and the number of cell pairs in each stage.

### 4.2 Visualization of Constraint Boundaries

To further understand the cost-optimal design, Figure 6 can be used to connect how changes in geometry over the domain affect key outputs. For this visualization, N1 is fixed at 13 and width is fixed at 2 cm while the length and N1 are varied. The visualization is a useful tool when considering how variations in external constraints (such as the maximum available voltage or pumping pressure) may change both the shape and cost of the ideal design.

#### 4.2.1 Discussion of Individual Outputs

The first parameter considered when exploring the design space was how the applied current density was affected by path length and cell pair counts. This is a technical constraint imposed on the system and therefore the boundary is immobile in the case of potential system improvements by the designer. Figure 6a shows the permissible and impermissible (shaded) regions of the design space as bounded by the constraint on $r_{ilim}$. For the same geometry, increasing the N2 cell pair count (moving up the vertical axis) decreases the amount of the path over $r_{ilim}$ by slowing the flow velocity. This type of system modification is possible to implement after a stack has been designed and is a notable point of flexibility.

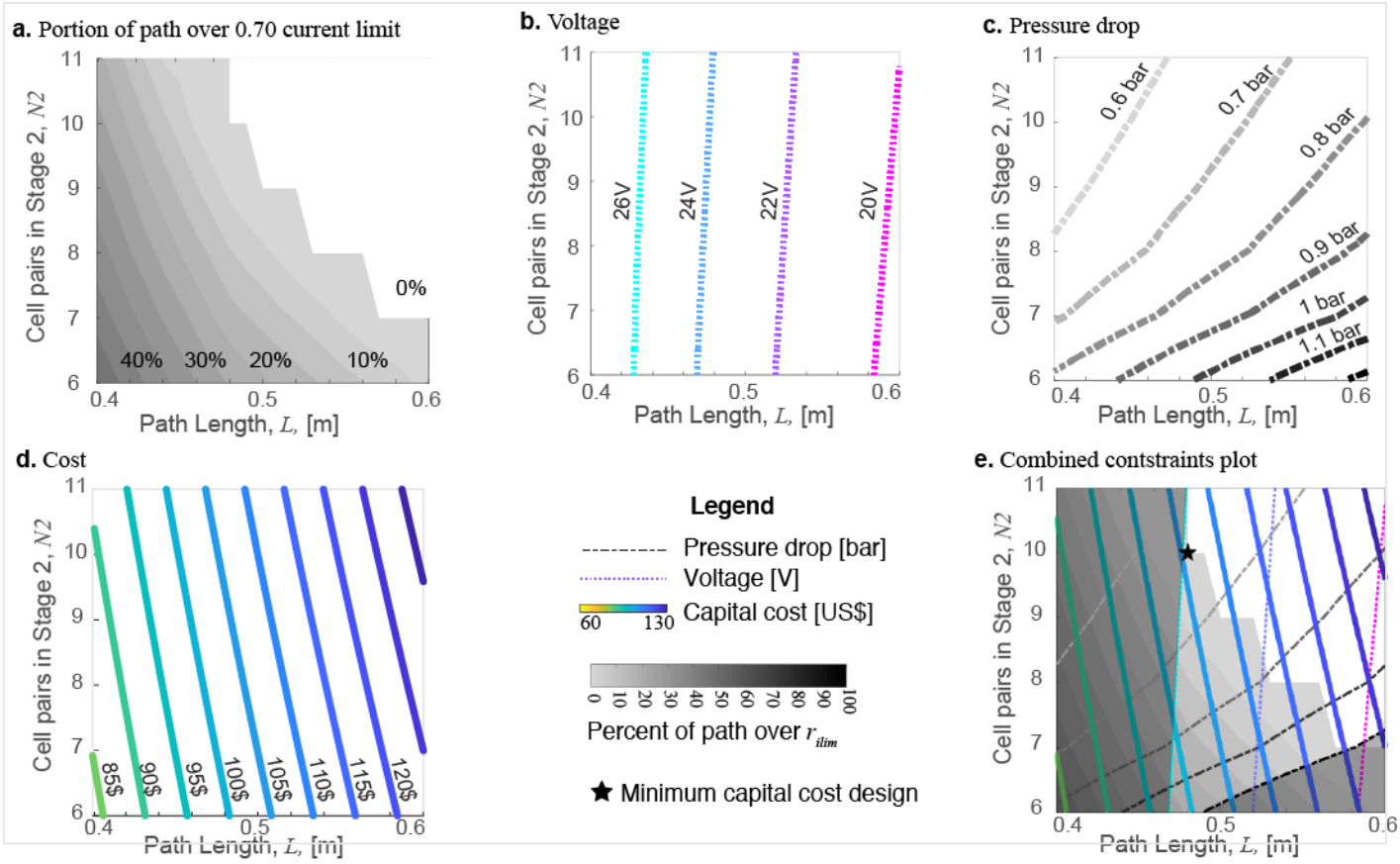


**FIGURE 6:** Design space exploration for a path width 20 mm, 13 cell pairs in the first stage **a.** Increasing active area decreases the amount of flow path over the applied current threshold **b.** Voltage decreases with lower cell pair series resistance or increased path length **c.** Pressure isobars show increasing pressure with geometric changes that increase channel flow velocity. **d.** Increasing the active area of a single cell pair has a greater effect on cost than increasing the number of cell pairs given the higher relative cost of the electrode compared to the membrane. **e**. The optimal design lies on the limiting current ratio constraint boundary. It includes 13 cell pairs in stage 1, 10 in stage 2, a path length of 0.48 [m], path width of 0.02 [m] and results in a capital cost of US$105.86 for membranes and electrodes. Path width 20 mm

Figure 6b shows that as active area per cell pair increases with growing length, the voltage required to achieve a target concentration also decreases. This occurs because a lower corresponding applied current density is required to remove the same salt. The slight vertical increase in voltage is required to overcome the increasing resistance with more cell pairs added to the second stage.

Given the relation of pressure to $u_v^2$ (Equation 2), it is reasonable that the lines of constant pressure shown in Figure 6c are sensitive to geometry changes that influence the void channel velocity and increase in proportion to longer flow paths or fewer channels. Again, a designer could modify a system design in this way in order to meet a change in the pressure constraint.

#### 4.2.2 Determination of Constraint-Bounded Minimum Cost Design

The performance of this design relative to constraints is visualized in Figure 6e. The constraints limits have been overlaid onto the composite plot as shaded regions. Voltage requirements over 24V would fall to the left-hand side of the plot, nearer the y-axis. Pressure drop predictions over 1 bar fall in the lower right portion of the plot and are also excluded. The only active constraint at this optimum is $r_{ilim}$. While the predicted voltage is close to the 24V limit, the constraint is not considered active because there is no feasible solution with a lower capital cost if only the applied current constraint is considered (i.e. relaxing the 24V limit does not affect the optimal design choice).

Access to the visual relations portrayed in Figure 6e allow for rapid assessment of the limiting factors in the design and where additional efforts should be focused to provide further reduction in capital cost. From this case study it is clear that neither the available pump or voltage supply impose a limit on cost, however examining the spacers within the stack may provide the best avenue of further development.

**TABLE 3.** Sensitivity of cost to nearby solution values. Active constraints may be in the form of voltage ($V$), pressure ($P$) or applied current ($i$)

| W [cm] | N1 | N2 | L [cm] | Average $i$ [Ωm$^2$] | Cost Increase [US$ (%)] | Active Constraint |
|---|---|---|---|---|---|---|
| 1.5 | 13 | 13 | 64 | 120 | 12.5 (11.8%) | *P, V* |
| 2.0 | 12 | 9 | 50 | 135 | 0.9 (0.8%) | *i* |
| **2.0** | **13** | **10** | **48** | **129** | **OPTIMAL** | ***i*** |
| 2.0 | 14 | 10 | 48 | 122 | 1.5 (1.5%) | *i, V* |
| 2.5 | 15 | 11 | 39 | 110 | 2.1 (2.0%) | *i, V* |

### 4.3 Sensitivity Analyses

#### 4.3.1 Cost Sensitivity to N1

The easiest geometric variable to adjust after a stack has been designed and manufactured is the cell pair count. This can be done to alter the pressure drop within the stack by varying linear flow velocity in the system. Given this flexibility, we examined the cost optimal configurations at N1 values that were above and below the cost optimal point. Adding one cell pair in the first stage did not change the cost-optimal length of the flow path or number of cell pairs required in stage 2 however it did increase the material cost by just over 1% as can be seen in Table 3. Reducing the number of cell pairs in the first stage led to a cost optimal design for meeting the performance requirements that has a slightly longer path and fewer cell pairs in the second stage. This design increased capital costs by around 1% however it would not be interchangeable with components from the original optimum.

#### 4.3.2 Cost Sensitivity to Flow Path Width

Pressure loss is also highly sensitive to flow path width for a given volumetric flow rate. In the case where pressure loss was known to be of concern, a wider path would be favorable to decrease this loss. Modifying the design width is a decision that would need made prior to fabrication as it drastically changes the flow path form (length and cell pair count). Here we examined what cost increase was derived from presetting the path widths 0.5 cm above and below the determined cost optimal width.

Table 3 details the capital cost increases with these changes as well as the optimal length for each. Figure 7 shows the constraint plot of these two configurations. Of note here are the active constraints for the new design widths: pressure drop and applied voltage limit the design for the 1.5 cm path width system (Figure 7a), whereas the 2.5 cm width case is limited by the current threshold (Figure 7b).

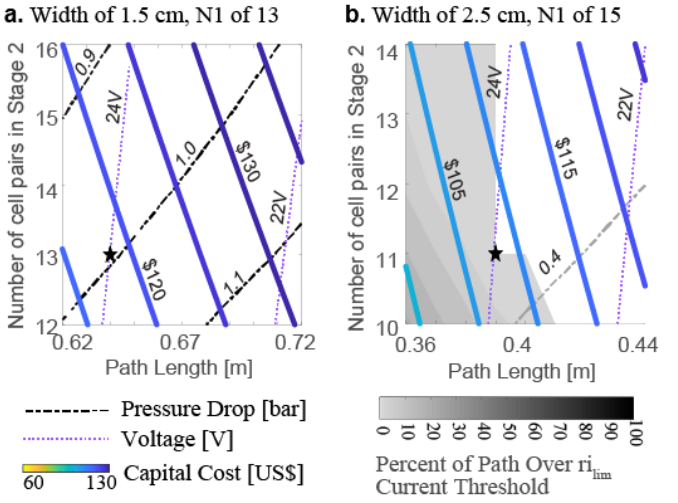


**FIGURE 7:** Feasible design solutions for varied path geometries. **a.** An inferior optimum is indicated as the design is limited by imposed constraints to require more cell pairs and greater length. **b.** Shows lower cost options but is limited by the applied current threshold.

When the flow path width is increased, $u_v$ decreases, therefore reducing the mixing within the channel and resulting in a lower limiting current density. In order to compensate for the lower applied current density, the total active area must increase through increasing the cell pair count or path length. This system would operate at a lower pressure than the 2 cm width cost-optimal design, which could be favorable in a low pressure (e.g. gravity fed) application.

In considering the case of decreased width, the maximum voltage constraint is active, forcing a longer path length in order to increase the active area of the system and decrease the applied current density. Pressure drop is also proportional to path length (per Equation 2), so the pressure drop constraint begins driving the addition of cell pairs in the design order to reduce the flow velocity. The capital cost of this design would be reduced if either the pressure or voltage constraints were relaxed, pointing to the potential need for a more powerful pump or voltage supply.

### 4.5 Validation of Analytical Midpoint Salinity Target

With the same feed salinity and path shape, we were able to validate the calculation from Section 3.3.1, which predicted that a 2-stage stack will have optimal performance when the intermediate concentration is the geometric mean of the feed and product concentrations. Figure 8 demonstrates this for the cost-optimal case previously described. Three path lengths were tested for 7, 10 and 13 cell pairs in the second stage and the intermediate concentration was incremented between the feed and product concentration. Allowing the simulation to apply the required voltage to achieve the target intermediate and feed salinities. For a given length flow path, the portion of the flow path operating above the $r_{ilim}$ threshold should be 0% at all times in order to ensure increased long-term reliability in operation.

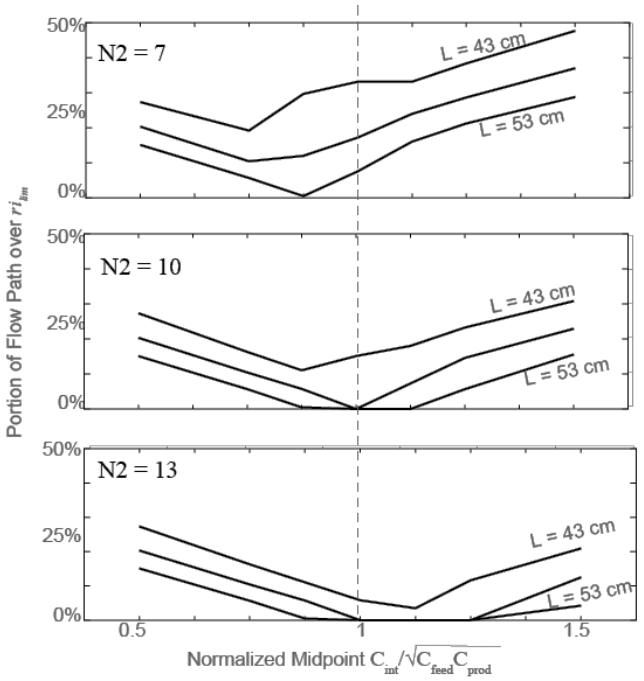


**FIGURE 8:** Manually varying the midpoint salinity show convergence on the geometric mean as the intermediate salinity with the least amount of flow path over the current threshold across a range of path lengths and number of cell pairs in the second stage (N2). Convergence is best at the optimal capital cost design (minimum membrane area). Path width 20 mm, 13 cell pairs in the first stage.

It can be seen in all cases that the least amount of the flow path was over the threshold applied current level when $C_{int}$ was near the geometric mean and the correlation is best when the number of cell pairs in the second stage represents the cost optimal design. For the higher and lower cell pair counts, the non-optimal cases favor increased amount of desalination in the stage that has a relative membrane 'surplus', shifting the inflection point to a higher intermediate salinity in the case of greater membrane area in stage 2 (N2=13), and lower $C_{int}$ when less membrane area is present (N2=7).

### 4.6 Limitations of the Design

Through the analyses presented here we have arrived at a possible design that is suitable for the POU market in India. The constraints and costs included are some of the key parameters in designing an electrodialysis stack, however they are only a subset of the full items that both constrain the design and add cost to a fielded unit. Additional costs for hydraulics, controls and housing would have to be considered in understanding the market viability of the product. Multiple stages will add component and control complexity and costs over a single stage, but simplicity when compared to batch, for example.

Key aspects of what make any consumer product viable, such as reliability, ease of use, and familiarity cannot be easily quantified in such an analysis. Mineral scaling and fouling are also concerns in ED systems that require experimental characterization. Hence, our next step for determining commercial viability will involve prototyping the device, testing it in the field, and receiving user feedback.

## 5. CONCLUSION

In this paper we present a potential architecture and design for a cost-optimal 2-stage continuous ED stack targeted at the Indian POU market. Through a simplified system architecture and detailed parameterized survey of the designs space, the proposed design has a capital cost below the retail price for current RO POU purifiers on the Indian market. At the same time it provides a significant new value proposition for a region that is facing water scarcity: conserving up to 90% of the feed water to the system. Further, the design provides continuous delivery of water, improving upon previously proposed POU ED systems that have primarily focused on batch water delivery.

Future work should explore fabricating and testing the proposed system, comparing performance predictions to the simulated results and validating the long-term performance of the proposed architecture. Sensitivity to feed salinity and salt reduction are additional parameters of interest that could be examined using a similar method as was employed here. As this design is further validated, future work should also expand on the limitations discussed in Section 4, in particular, mineral scale mitigation. There is a great opportunity for POU water purifiers in the Indian domestic market that provide more efficient desalination to customers; the system design presented here is a building block towards making ED desalination a reality in this setting.

## ACKNOWLEDGEMENTS

This work was supported by Eureka Forbes Ltd., India.

## REFERENCES

[1] Wright, N. C., and Winter, A. G., 2014, "Justification for Community-Scale Photovoltaic-Powered Electrodialysis Desalination Systems for Inland Rural Villages in India," Desalination, **352**, pp. 82–91.

[2] Frost and Sullivan, 2018, *Indian Water Purifiers Market, FY2018. PA12-25*.

[3] Comprehensive Initiative on Technology Evaluation at MIT, 2015, "Household Water Filter Evaluation," pp. 1–64.

[4] Oren, Y., Korngold, E., Daltrophe, N., Messalem, R., Volkman, Y., Aronov, L., Weismann, M., Bouriakov, N., Glueckstern, P., and Gilron, J., 2010, "Pilot Studies on High Recovery BWRO-EDR for near Zero Liquid Discharge Approach," Desalination, **261**(3), pp. 321–330.

[5] Bakker, K., 2003, "Archipelagos and Networks: Urbanization and Water Privatization in the South," Geogr. J., **169**(4), pp. 328–341.

[6] Kaur, B., 2019, "Ban RO Systems If Dissolved Solids Are Less than 500 Mg/l: NGT," DownToEarth [Online]. Available: https://www.downtoearth.org.in/news/water/ban-ro-systems-if-dissolved-solids-are-less-than-500-mg-l-ngt-64795. [Accessed: 24-Feb-2020].

[7] Connor, C. L. O., 2016, "Decentralized Water Treatmen in Urban India, and the Potential Impacts of Reverse Osmosis Water Purifiers."

[8] Nayar, K. G., Sundararaman, P., O'Connor, C. L., Schacherl, J. D., Heath, M. L., Gabriel, M. O., Shah, S. R., Wright, N. C., and Winter, V, A. G., 2016, "Feasibility Study of an Electrodialysis System for In-Home Water Desalination in Urban India," Dev. Eng., **2**(December 2016), pp. 38–46.

[9] Thampy, S., Desale, G. R., Shahi, V. K., Makwana, B. S., and Ghosh, P. K., 2011, "Development of Hybrid Electrodialysis-Reverse Osmosis Domestic Desalination Unit for High Recovery of Product Water," Desalination, **282**, pp. 104–108.

[10] Campione, A., Gurreri, L., Ciofalo, M., Micale, G., Tamburini, A., and Cipollina, A., 2018, "Electrodialysis for Water Desalination: A Critical Assessment of Recent Developments on Process Fundamentals, Models and Applications," Desalination, **434**(December 2017), pp. 121–160.

[11] Murray, P., 1995, *Electrodialysis and Electrodialysis Reversal - Manual of Water Supply Practices, M38 (1st Edition)*.

[12] He, W., Amrose, S., Wright, N. C., Buonassisi, T., Peters, I. M., and Winter, A. G., 2018, "Field Demonstration of a Cost-Optimized Solar Powered Electrodialysis Reversal Desalination System in Rural India," Desalination, **476**.

[13] Government of India, 2010, *Central Ground Water Board, Ground Water Quality in Shallow Aquifers of India*.

[14] Consumer Voice, 2016, "Packaged Drinking Water / Mineral Water."

[15] Wright, N. C., Shah, S. R., Amrose, S. E., and Winter, A. G., 2018, "A Robust Model of Brackish Water Electrodialysis Desalination with Experimental Comparison at Different Size Scales," Desalination, **443**(April), pp. 27–43.

[16] Ponzio, F. N., Tamburini, A., Cipollina, A., Micale, G., and Ciofalo, M., 2017, "Experimental and Computational Investigation of Heat Transfer in Channels Filled by Woven Spacers," Int. J. Heat Mass Transf., **104**, pp. 163–177.

[17] Ortiz, J. M. M., Sotoca, J. A. A., Expósito, E., Gallud, F., García-García, V., Montiel, V., and Aldaz, A., 2005, "Brackish Water Desalination by Electrodialysis: Batch Recirculation Operation Modeling," J. Memb. Sci., **252**(1–2), pp. 65–75.

[18] Fidaleo, M., and Moresi, M., 2011, "Electrodialytic Desalting of Model Concentrated NaCl Brines as Such or Enriched with a Non-Electrolyte Osmotic Component," J. Memb. Sci., **367**(1–2), pp. 220–232.

[19] 2014, *Hangzhou Iontech Environmental Co. Ltd, IONSEP Membranes.*, Zhejiang, China.

[20] 2014, *Baoji Changli Special Metal Co. Ltd, Platinized Titanium Anode*, Shaanxi, China.

[21] Shah, S. R., Walter, S. L., and Winter, A. G., 2019, "Using Feed-Forward Voltage-Control to Increase the Ion Removal Rate during Batch Electrodialysis Desalination of Brackish Water," Desalination, **457**, pp. 62–74.

## APPENDIX 1. Intermediate Concentration Target

Assuming the total active area required is the sum of the area in the first and second stage, the optimal intermediate concentration, $C_I$, can be found by taking the partial derivative of total area with respect to $C_I$ per Equation A.1.

$$\frac{\partial A_{Total}}{\partial C_I} = \frac{\partial A_1}{\partial C_I} + \frac{\partial A_2}{\partial C_I} = 0 \tag{A.1}$$

Equation A.2, below gives an approximate ratio of feed to product concentration for any stage given a total membrane area ($WLN$), open area porosity of the spacer ($\eta$), threshold ratio of applied to limiting current ($r_i$), minimum of the ion transport numbers between cation and anions in the solution ($t^{+/-}$) here taken as $t^+ = 0.39$ for $Na^+$, flow rate per cell pair ($Q_{cp}$) and diffusion coefficient ($k$). Refer to Shah et al. for the assembly of these variables into relation used here[21].

$$\frac{C_{feed}}{C_{prod}} = 1 + \frac{\eta r_i WLNk}{Q_{cp}(1-t^{+/-})} \tag{A.2}$$

$$\frac{C_{feed}}{C_{prod}} - 1 = \frac{R\,A}{\sqrt{NW}} \tag{A.3}$$

With consistent spacer material properties this simplifies to an equation relating area to the desalination ratio with a constant prefactor ($R$) per Equation A.3. Noting that the intermediate concentration of the full ED stack will be the *product* of stage 1 and the *feed* into stage 2, Equation A.1 can be used to determine the full relationship of $C_{feed}$, $C_I$, and $C_{prod}$ as the geometric mean:

$$C_{int} = \sqrt{C_{feed} C_{prod}} \quad \text{(A.3.)}$$